Electron-impact ionization of Si^{6+} and Si^{7+} ions

P. A. Zeijlmans van Emmichoven,* M. E. Bannister, D. C. Gregory, C. C. Havener, and R. A. Phaneuf†
Oak Ridge National Laboratory, Oak Ridge, Tennessee 37831-6372

E. W. Bell, X. Q. Guo, and J. S. Thompson†
Joint Institute for Laboratory Astrophysics, University of Colorado, Boulder, Colorado 80309-0440

M. Sataka
Department of Physics, Japan Atomic Energy Research Institute, Tokai-mura, Ibaraki, 319-11, Japan
(Received 30 October 1992)

Crossed beams of electrons and ions have been used to measure absolute cross sections for single ionization of Si^{6+} and Si^{7+} ions from below threshold to 1400 eV. The measurements for Si^{6+} and Si^{7+} agree with distorted-wave calculations for direct ionization within 20% and 5%, respectively, suggesting that this mechanism is the dominant contribution to the cross section. The bulk of the measurements were performed with the more abundant ^{28}Si isotope; however, due to beam impurities, measurements with ^{29}Si were used to correct the ^{28}Si data.

PACS number(s): 34.80.Kw

I. INTRODUCTION

Natural and laboratory plasmas are topics of current experimental and theoretical interest [1,2]. Absolute cross sections for electron-impact ionization, excitation, and recombination of a wide variety of ions found in plasmas are needed to estimate rate coefficients used in plasma modeling codes.

To date many experiments and calculations have been performed on electron-impact single ionization of multicharged ions [3]. *Direct* ionization, which may be thought of as a knock-on collision between the incident electron and a target electron, is the simplest and often dominant contributing mechanism [4]. Distorted-wave calculations using the first Born approximation have been shown to be very useful in predicting the absolute cross section for direct ionization [5–7]. Recently, the asymptotic behavior of the final-state wave functions used in the distorted-wave method has been investigated for the electron ionization of helium atoms in an effort to better model the interactions between the two outgoing electrons [8,9].

Electron-impact-ionization measurements and calculations for numerous systems have shown that *indirect* mechanisms may also play an important role in the single ionization of multicharged ions [4,10,11]. One important example is excitation-autoionization, in which the incident electron excites an inner-shell electron into an autoionizing state of the ion. For ions with only a few electrons in the outermost shell, strong contributions from this indirect mechanism have been observed. One example is the isonuclear sequence of Xe [4,12]. For Xe^{2+} the ionization cross section is dominated by direct ionization. As the charge of the ions increases, the contribution of excitation-autoionization to the total cross section increases, leading to dominance over direct ionization for Xe^{5+} and Xe^{6+}.

Although the absolute cross section for electron-impact ionization has been measured for many ions likely to be found in the plasma edge of fusion reactors, a significant number of elements have not yet received a great deal of attention [3]. In the silicon sequence, for example, only the ionization cross section of sodiumlike Si^{3+} has been previously studied [13]. In this case, contributions from both direct ionization and excitation-autoionization were observed. A series of measurements of absolute cross sections for other charge states of silicon has been initiated at Oak Ridge National Laboratory (ORNL). In this paper we report on the measurements for oxygenlike Si^{6+} and nitrogenlike Si^{7+}, and compare the results with configuration-averaged distorted-wave calculations for direct ionization [14].

II. EXPERIMENT

The crossed-beams apparatus and the experimental technique have been described in detail elsewhere [15], and only a brief description of the main characteristics will be given here. A schematic drawing of the experimental setup is shown in Fig. 1. The background pressure during the measurements was roughly 10^{-7} Pa. The ions are extracted from the Oak Ridge National Laboratory Electron Cyclotron Resonance (ORNL ECR) ion source [16] at 10 kV and analyzed by a 90° magnetic charge analyzer. After charge purification by a parallel-plate analyzer, the ions are crossed with a magnetically confined electron beam which is chopped at 50 Hz. Profiles of the ion and electron beams are measured with a moving-slit beam probe which is located in the center of the collision region. The electrons are collected by a biased array of edge-forward tantalum "razor blades" to minimize reflection. The product ions $Si^{(q+1)+}$ are dispersed from the primary ion beam (Si^{q+}) by a double-focusing magnet located downstream of the collision re-

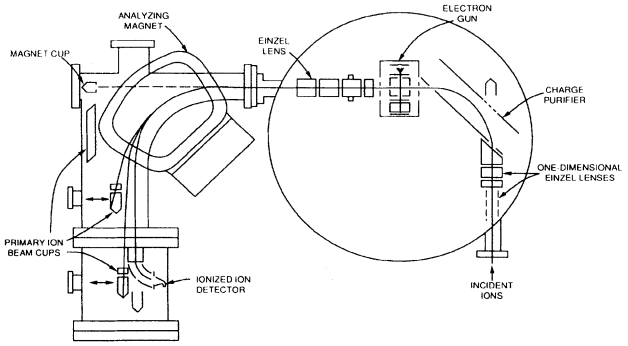

FIG. 1. Crossed-beams experimental apparatus. See text for explanation.

gion. The magnetic field is set such that the $Si^{(q+1)+}$ product ions are deflected by 90° into an electrostatic deflector used to direct the ions onto a channel electron multiplier. Several Faraday cups are available for the detection of the primary Si^{q+} ion beam, the cup used depending on the angle of deflection by the analyzing magnetic field for that particular final to initial charge ratio.

The absolute cross section is determined [17] from the measurements as follows:

$$\sigma(E)=\frac{R}{I_i I_e}\frac{qe^2 v_i v_e}{(v_i^2+v_e^2)^{1/2}}\frac{F}{D}\ , \tag{1}$$

with $\sigma(E)$ the absolute cross section at electron-impact energy E, R the product ion count rate, I_i and I_e the incident ion and electron currents, q the charge state of the incident ions, e the electronic charge, v_i and v_e the incident ion and electron velocities, respectively, F the form factor which is determined from the two beam profiles, and D the detection efficiency for the product ions which we estimated at 98% [18].

A. Purity of ion beams

The magnetic analyzer used to select beams from the ECR ion source does not separate $^{28}Si^{6+}$ from $^{14}N^{3+}$ since these ions have the same mass-per-charge ratio. Contamination of the source plasma with N_2 therefore may give rise to $^{14}N^{3+}$ ions in the primary ion beam. This would affect the measured cross sections for $^{28}Si^{6+}$ due to the portion of $^{14}N^{3+}$ ions detected at the primary ion-beam cup. The detected product ions consist only of $^{28}Si^{7+}$ because the mass per charge is different from that of the product ions from $^{14}N^{3+}$. The effect of $^{14}N^{3+}$ impurities in the ion beam is therefore a reduction in the measured cross section.

Different data sets of relative cross sections were measured with $^{28}Si^{6+}$ ions. Each data set, with approximately constant source conditions, included an electron-impact energy of 640 eV. At this energy the absolute cross section was measured for $^{29}Si^{6+}$, the second most abundant isotope of silicon (4.67% [19]). This measurement was rather time consuming due to a relatively low ion-beam intensity, which was, however, not affected by beam impurities. The ratio of the cross sections taken at 640 eV for $^{28}Si^{6+}$ and $^{29}Si^{6+}$ yields the purity fraction of the $^{28}Si^{6+}$ ion-beam *current*. For different data sets this $^{28}Si^{6+}$ purity fraction ranged from (0.354 ± 0.017) to (0.758 ± 0.021) corresponding to different ion-source vacuum conditions. The relative uncertainties of these purity fractions are given at the one-standard-deviation level and only take into account counting statistics of the measurements performed with the two isotopes. These values have been used to correct for impurities in the primary ion-beam currents for measurements with $^{28}Si^{6+}$.

For $^{28}Si^{7+}$ similar problems as described for $^{28}Si^{6+}$ arise due to overlap in mass per charge with $^{16}O^{4+}$. The different data sets of relative cross sections were taken with $^{28}Si^{7+}$, always including an electron-impact energy of 640 eV. The purity fraction of the ion beam was obtained from the relative and absolute cross sections at 640 eV. The absolute cross section at 640 eV was taken as the reciprocal-variance-weighted average of the absolute cross sections measured in two different ways. The first method uses a pure $^{29}Si^{7+}$ ion beam as discussed for $^{28}Si^{6+}$, the second uses a $^{28}Si^{7+}$ beam, with the fraction of contamination by $^{16}O^{4+}$ estimated from a linear interpolation between the measured intensities for $^{16}O^{3+}$ and $^{16}O^{5+}$. The absolute cross sections determined with these two methods differ by less than the sum of their relative uncertainties at the one-standard-deviation level. The purity fraction of the primary ion-beam currents for different data sets ranged from (0.757 ± 0.045) to (1.000 ± 0.056) corresponding to different ion-source conditions. The relative uncertainties in these fractions were obtained in a similar way as described for Si^{6+}. These values have been used to correct for impurities in the primary ion-beam currents.

B. Uncertainties

Relative uncertainties at the one-standard-deviation level are obtained from the quadrature sum of counting statistics and the relative uncertainty in the purity fraction of the ion beam. The variation of the form factor during each measurement was found to be negligible and is therefore not included in the relative uncertainties. The total absolute uncertainty of the cross section is obtained from the quadrature sum of the uncertainties of the measured quantities occurring in Eq. (1), including the relative uncertainty discussed above. Tables with absolute uncertainties for these quantities have been published elsewhere [20]. For the experiments discussed here the absolute uncertainty excluding relative uncertainties is about 7% at good confidence level, i.e., at the two-standard-deviation level. The total uncertainty of the absolute cross section at good confidence level at electron-impact energies above 600 eV ranges from 9% to 12% for Si^{6+} and from 12% to 17% for Si^{7+}.

III. RESULTS

Measured absolute cross sections with relative uncertainties at the one-standard-deviation level for single ionization of Si^{6+} and Si^{7+} ions are shown as functions of electron-impact energy in Tables I and II, and Figs. 2 and

3 in the energy range 0 to 1400 eV. Also shown in the figures are distorted-wave calculations for the absolute cross section for direct ionization of $Si^{6+}(1s^22s^22p^4)$ and $Si^{7+}(1s^22s^22p^3)$ [14]. Details of calculating electron-impact-ionization cross sections in the configuration-averaged distorted-wave (CADW) approximation have been published elsewhere [7]. The CADW calculations used configuration-averaged ionization energies calculated with Cowan's Hartree-Fock code [21] for the $2s$ and $2p$ electrons. The calculated ionization energies for $2p$ and $2s$ electrons are 252 and 295 eV for Si^{6+}, and 299 and 336 eV for Si^{7+}, respectively. The ionization energy of the $1s$ electron is about 2 keV for both ions, and thus does not contribute to the direct-ionization channel in the energy interval studied.

Comparison of the measurements and CADW predictions suggests that electron-impact single ionization of Si^{6+} and Si^{7+} ions is dominated by direct ionization. This was also observed for electron-impact ionization of the respective isoelectronic Ne^{2+} and Ne^{3+} ions [18,22].

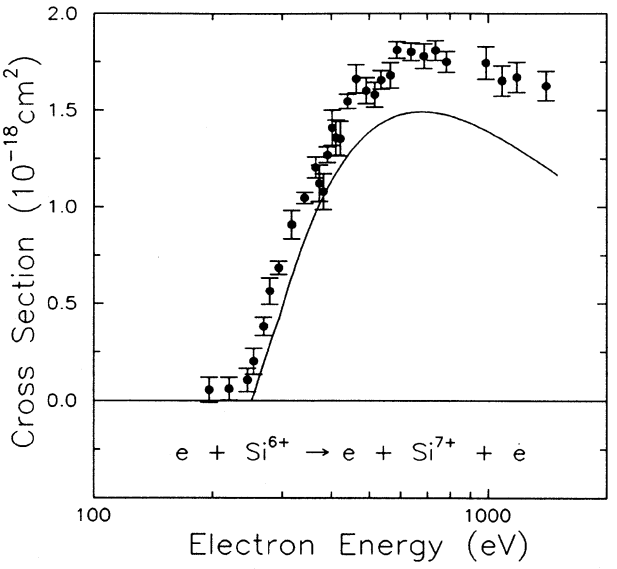

FIG. 2. Absolute cross sections as a function of electron-impact energy for single ionization of Si^{6+}. The present experimental results are indicated by solid circles. Relative uncertainties are shown at the one-standard-deviation level. Results of distorted-wave calculations are indicated by the solid curve (Ref. [14]).

TABLE I. Absolute cross sections for electron-impact single ionization of Si^{6+}. The relative uncertainties are given at the one-standard-deviation level. Absolute uncertainties at two-standard-deviation level are given in parentheses and are obtained from the quadrature sum of twice the relative uncertainties given and 7% from the other measured quantities in Eq. (1).

E (eV)	σ (10^{-18} cm^2)
196	0.056±0.064(0.128)
220	0.061±0.058(0.116)
245	0.106±0.060(0.120)
254	0.202±0.067(0.135)
269	0.382±0.047(0.098)
279	0.564±0.068(0.142)
294	0.685±0.034(0.083)
317	0.909±0.073(0.159)
342	1.047±0.029(0.093)
365	1.206±0.054(0.137)
373	1.123±0.094(0.204)
382	1.080±0.093(0.201)
391	1.271±0.041(0.121)
402	1.410±0.091(0.207)
411	1.359±0.090(0.204)
421	1.354±0.089(0.202)
440	1.546±0.037(0.131)
463	1.662±0.073(0.187)
491	1.601±0.067(0.175)
516	1.580±0.064(0.169)
536	1.656±0.048(0.151)
566	1.680±0.066(0.177)
588	1.811±0.043(0.153)
638	1.802±0.046(0.156)
687	1.779±0.064(0.179)
735	1.809±0.051(0.163)
784	1.750±0.054(0.163)
987	1.745±0.084(0.208)
1085	1.652±0.078(0.194)
1183	1.670±0.078(0.195)
1403	1.626±0.076(0.190)

TABLE II. Absolute cross sections for electron-impact single ionization of Si^{7+}. The relative uncertainties are given at the one-standard-deviation level. Absolute uncertainties at two-standard-deviation level are given in parentheses and are obtained from the quadrature sum of twice the relative uncertainties given and 7% from the other measured quantities in Eq. (1).

E (eV)	σ (10^{-18} cm^2)
200	0.019±0.072(0.144)
249	−0.009±0.115(0.230)
298	0.004±0.047(0.094)
323	0.127±0.046(0.092)
347	0.298±0.033(0.069)
372	0.355±0.044(0.091)
386	0.397±0.065(0.133)
396	0.500±0.036(0.080)
421	0.552±0.045(0.098)
445	0.662±0.040(0.092)
470	0.642±0.037(0.087)
494	0.756±0.059(0.129)
519	0.781±0.067(0.145)
544	0.826±0.041(0.100)
593	0.860±0.067(0.147)
642	0.877±0.040(0.101)
740	0.917±0.055(0.127)
789	0.878±0.069(0.151)
888	0.952±0.056(0.130)
986	0.890±0.064(0.142)
1182	0.821±0.057(0.128)
1363	0.812±0.056(0.126)

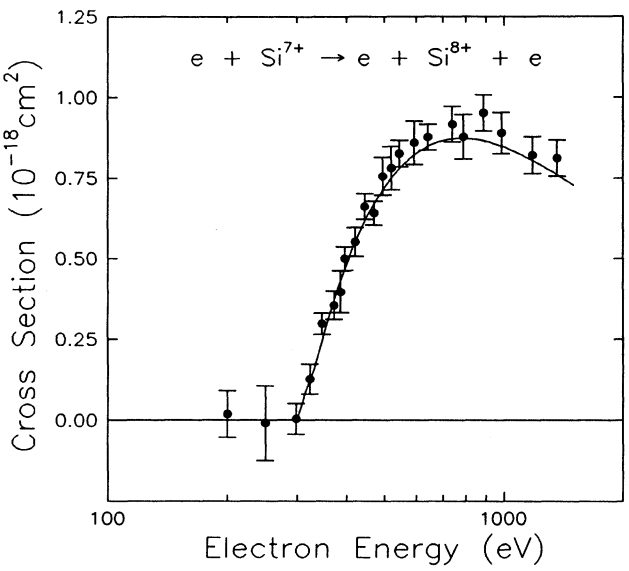

FIG. 3. Absolute cross sections as a function of electron-impact energy for single ionization of Si^{7+}. The present experimental results are indicated by solid circles. Relative uncertainties are shown at the one-standard-deviation level. Results of distorted-wave calculations are indicated by the solid curve (Ref. [14]).

The measurements for Si^{6+} show slight evidence for structure in the range of electron-impact energies from 400 to 600 eV. Such structure typically indicates contributions from indirect channels. For Si^{6+}, however, indirect channels such as excitation-autoionization seem very unlikely because the energies at which structure is observed are too high for excitation of a $2s$ electron (above ionization threshold) and too low for excitation of a $1s$ electron. No evidence of any structure is observable for Si^{7+}. For Si^{6+} the CADW predictions are approximately 20% below the measured values while for Si^{7+} the CADW predictions are roughly 5% lower. It should be noted that the Lotz one-parameter formula [23] agrees with the CADW calculations to within 5% for both Si^{6+} and Si^{7+}.

The measured cross sections at electron-impact energies below the predicted onsets for ionization from the ground states give an indication of the possible presence of metastable ions in the reactant beams (see onsets of the CADW curves in Figs. 2 and 3). For Si^{6+} a fraction of metastables with different electronic configurations (e.g., $1s^2 2s 2p^5$) may contribute to the measured cross section and may be responsible for the measured cross section being 20% larger than the CADW calculations. For Si^{7+} the measurements show no evidence of contributions from metastables.

ACKNOWLEDGMENTS

We are indebted to M. S. Pindzola for providing us with the distorted-wave calculations and insights into the theory of electron-ion collisions. We are also grateful to G. H. Dunn, F. W. Meyer, and A. C. H. Smith for stimulating discussions and to J. Hale for his skilled technical assistance. In addition, we thank N. Djurić for calculating the rate coefficients and fitting parameters. This work was supported by the Office of Fusion Energy, U. S. Department of Energy, under Contract No. DE-AC05-84OR21400 with Martin Marietta Energy Systems, Inc. M. E. B. received support from the DOE Laboratory Cooperative Postgraduate Research Training Program administered by Oak Ridge Associated Universities. P.A.Z.v.E. received support from the Joint Institute for Heavy Ion Research, Holifield Heavy Ion Research Facility.

TABLE III. Maxwellian rate coefficients (in units of cm^3/s) for the ionization of Si^{6+} and Si^{7+} at selected values of T (in K) calculated from the measured cross sections (see Appendix).

Electron temperature	Ionization rate coefficients α (cm^3/s)	
T (K)	Si^{6+}	Si^{7+}
1.0×10^5	4.28×10^{-20}	4.56×10^{-25}
2.0×10^5	3.33×10^{-15}	1.50×10^{-17}
4.0×10^5	1.77×10^{-12}	1.27×10^{-13}
6.0×10^5	1.84×10^{-11}	2.81×10^{-12}
8.0×10^5	6.28×10^{-11}	1.36×10^{-11}
1.0×10^6	1.35×10^{-10}	3.57×10^{-11}
2.0×10^6	6.66×10^{-10}	2.59×10^{-10}
4.0×10^6	1.58×10^{-9}	7.21×10^{-10}
6.0×10^6	2.16×10^{-9}	1.01×10^{-9}
8.0×10^6	2.54×10^{-9}	1.20×10^{-9}
1.0×10^7	2.81×10^{-9}	1.32×10^{-9}
2.0×10^7	3.40×10^{-9}	1.55×10^{-9}
4.0×10^7	3.61×10^{-9}	1.59×10^{-9}
6.0×10^7	3.58×10^{-9}	1.54×10^{-9}
8.0×10^7	3.50×10^{-9}	1.49×10^{-9}
1.0×10^8	3.41×10^{-9}	1.44×10^{-9}

APPENDIX: RATE COEFFICIENTS

For many applications such as plasma modeling, it is useful to report Maxwellian rate coefficients for the process investigated. Table III lists rate coefficients calculat-

TABLE IV. Rate-coefficient fitting parameters. All parameters are in units of 10^{-15} $cm^3\,K^{-1/2}\,s^{-1}$. Rate coefficients in the range $10^5\,K \le T \le 10^8\,K$ may be calculated using these parameters in a Chebyshev polynomial expansion, or through Clenshaw's algorithm (see Appendix).

Fitting parameter	Si^{6+}	Si^{7+}
a_0	1648.96	641.257
a_1	−127.945	75.0597
a_2	−419.445	−333.790
a_3	−50.4497	23.1258
a_4	188.404	105.003
a_5	−69.4733	−38.7064
a_6	−7.759 55	−13.4105
a_7	19.042 9	13.9309
a_8	−7.718 38	−2.571 81
a_9	0.000 00	−1.690 28
a_{10}	0.000 00	0.933 665

ed from our present cross-section measurements using a method described elsewhere [24]. In addition, the rate coefficients were fit with Chebyshev polynomials of the first kind $T_n(x)$ to enable the user to calculate them for any temperature in the range $10^5\ \mathrm{K} \le T \le 10^8\ \mathrm{K}$:

$$\alpha(T)=T^{1/2}e^{-(I/kT)}\sum_{j=0}^{n} a_j T_j(x)\ , \tag{A1}$$

where I is the ionization potential. The coefficients $a_0 \ldots a_{10}$ given in Table IV reproduce the rate coefficients to within 1% over the given temperature range. The rate coefficient $\alpha(T)$ can be expressed simply as

$$\alpha(T)=\tfrac{1}{2}T^{1/2}e^{-(I/kT)}(b_0-b_2)\ , \tag{A2}$$

with the coefficients b_0 and b_2 calculated using Clenshaw's algorithm [25]:

$$b_j=2xb_{j+1}-b_{j+2}+a_j\ ,\quad j=0,1,2\ldots 10\ , \tag{A3}$$

where $b_{11}=b_{12}=0$ and the reduced energy x is given by

$$x=\frac{\log_{10}T-6.5}{1.5}\ . \tag{A4}$$

*Present address: Departamento de Fisica de Materiales, Facultad de Ciencias Químicas, Universidad del Pais Vasco, 20080 San Sebastian, Spain.

†Present address: Physics Department/220, University of Nevada, Reno, NV 89557.

[1] *Carbon and Oxygen Collision Data for Fusion Plasma Research,* Proceedings of a Specialists' Meeting of the International Atomic Energy Agency, Vienna, 1988, edited by R. K. Janev [Phys. Scr. **T28**, 5 (1989)].

[2] *Collision Processes of Metallic Ions in Fusion Plasmas,* Proceedings of an Advisory Group Meeting of the International Atomic Energy Agency, Vienna, 1990, edited by R. K. Janev [Phys. Scr. **T37**, 8 (1991)].

[3] G. H. Dunn, Nucl. Fusion Suppl. **2**, 25 (1992).

[4] R. A. Phaneuf, in *Atomic Processes in Electron-Ion and Ion-Ion Collisions,* edited by F. Brouillard (Plenum, New York, 1986), pp. 117–156.

[5] S. M. Younger, Phys. Rev. A **22**, 111 (1980).

[6] H. Jakubowicz and D. L. Moores, J. Phys. B **14**, 3733 (1981).

[7] M. S. Pindzola, D. C. Griffin, and C. Bottcher, in *Atomic Processes in Electron-Ion and Ion-Ion Collisions,* edited by F. Brouillard (Plenum, New York, 1986), pp. 75–91.

[8] C. Pan and H. P. Kelly, Phys. Rev. A **41**, 3624 (1990).

[9] J. Botero and J. H. Macek, Phys. Rev. Lett. **68**, 576 (1992).

[10] M. S. Pindzola, D. C. Griffin, and C. Bottcher, in *Electronic and Atomic Collisions,* edited by H. B. Gilbody, W. R. Newell, F. H. Read, and A. C. H. Smith (North-Holland, Amsterdam, 1988), pp. 129–145.

[11] A. Müller, Comm. At. Mol. Phys. **27**, 1 (1991).

[12] D. C. Griffin, C. Bottcher, M. S. Pindzola, S. M. Younger, D. C. Gregory, and D. H. Crandall, Phys. Rev. A **29**, 1729 (1984).

[13] D. H. Crandall, R.A. Phaneuf, R. A. Falk, D. S. Belić, and G. H. Dunn, Phys. Rev. A **25**, 143 (1982).

[14] M. S. Pindzola (private communication).

[15] D. C. Gregory, L. J. Wang, F. W. Meyer, and K. Rinn, Phys. Rev. A **35**, 3256 (1987).

[16] F. W. Meyer, Nucl. Instrum. Methods B **9**, 532 (1985).

[17] See, for example, M. F. A. Harrison, J. Appl. Phys. **17**, 371 (1966).

[18] D. C. Gregory, P. F. Dittner, and D. H. Crandall, Phys. Rev. A **27**, 724 (1983).

[19] *Handbook of Chemistry and Physics,* 67th ed., edited by R. C. Weast, M. J. Astle, and W. H. Beyer (CRC, Boca Raton, FL, 1986).

[20] See, for example, D. C. Gregory, F. W. Meyer, A. Müller, and P. Defrance, Phys. Rev. A **34**, 3657 (1986).

[21] R. D. Cowan, *The Theory of Atomic Structure and Spectra* (University of California Press, Berkeley, 1981).

[22] A. Danjo, A. Matsumoto, S. Ohtani, H. Suzuki, H. Tawara, K. Wakiya, and M. Yoshino, J. Phys. Soc. Jpn. **53**, 4091 (1984).

[23] W. Lotz, Z. Phys. **216**, 241 (1968).

[24] D. H. Crandall, G. H. Dunn, A. Gallagher, D. G. Hummer, C. V. Kunasz, D. Leep, and P. O. Taylor, Astrophys. J. **191**, 789 (1974).

[25] C. W. Clenshaw, Math. Tables Comput. **9**, 118 (1955).